Sampling the Configuration Space of Finite Atomic Systems: How Ergodic Is Molecular Dynamics?

F. Calvo,* J. Galindez, and F. X. Gadéa

Laboratoire de Physique Quantique, IRSAMC, Université Paul Sabatier, 118 Route de Narbonne, F31062 Toulouse Cedex, France

Received: October 3, 2001; In Final Form: February 8, 2002

We compare the efficiencies of deterministic molecular dynamics (MD) and Monte Carlo (MC) methods for sampling the configuration space of finite atomic systems, in both the microcanonical and canonical ensembles. By the examples of a nonlinear molecule, Ar_3, and a linear molecule, Ar_3^+, and several physical observables such as the absorption spectrum or the average kinetic energy release in unimolecular dissociation, we show that MD sampling can exhibit significant differences with respect to MC results. At low energy or low temperature, regular orbits and vanishing Lyapunov exponents prevent Newtonian MD from being ergodic. Also, a larger effect is observed because of angular momentum conservation, which is neglected in conventional MC. We show how the use of a suitable MC scheme can notably improve the ergodic properties of Newtonian molecular dynamics sampling.

I. Introduction

The increasing development of realistic simulations for molecular systems, including liquids, solids, biomolecules, and clusters, has emphasized the wide interest and need for high quality sampling of the phase space. The dynamical or statistical study of multidimensional potential energy surfaces (PES) is often conveniently performed by numerical simulation of the atomic or molecular system.[1,2] Molecular dynamics (MD) and Monte Carlo (MC) methods are commonly used to sample the configuration space but are very different in essence. Standard, deterministic MD follows the dynamical trajectory of the real system by solving the equations of motion. On the other hand, MC is a stochastic approach where only the equilibrium distribution of phase space points is meaningful. For some purposes, it can also be helpful to incorporate some stochastic elements in MD simulations (as in Langevin molecular dynamics) or some guiding elements to MC simulations (as in force-bias Monte Carlo). Usually, such a mixing results in the short-time dynamics being no longer physically relevant. Obviously, the need for measuring actual dynamical quantities in simulation requires one to choose MD methods over stochastic techniques. On the other hand, the sampling required for observables cast as a statistical problem can be equally obtained from MC or MD methods. However, the physical parameters and statistical ensembles come into play and may affect this choice. For instance, when simulating a bulk system at constant pressure or temperature, the numerical integrators required by adding extra degrees of freedom for the thermostat are generally of a higher order than those for constant energy systems, or they require shorter time steps. By comparison, Monte Carlo methods are relatively straightforward to implement.

Although the situation described above is still somewhat system-dependent, finite systems exhibit specific peculiarities which can bring difficulties when sampling the phase space. First, at sufficiently low energy, a Hamiltonian system will display regular trajectories. This behavior predicted by the Kolmogorov−Arnold−Moser (KAM) theorem occurs when only a small perturbation is applied. As the number of degrees of freedom increases, the KAM energy threshold will decrease rapidly. However, for molecules or small clusters, this threshold can be quite large, and the dynamics can be regular in a reasonably wide energy range. Regular molecular dynamics trajectories are not ergodic and should not be used for ergodic sampling. Second, the statistical ensembles sampled by MD and MC methods are not rigorously the same, regardless of whether energy or temperature is the conserved parameter. The difference is due to the conservation of angular momentum and is characteristic of finite atomic and molecular systems. At constant total energy, the microcanonical ensemble (NVE) is thus replaced by another ensemble where the angular momentum vector is prescribed to be $\vec{J}$ in addition to the number of particles N, volume V, and energy E. The NVE $\vec{J}$ ensemble is called the molecular dynamics ensemble and has been devoted a few studies in the past.[3−7] At constant temperature, extended systems which include thermostat variables also conserve angular momentum when it is set to zero. While regular trajectories are less likely to occur because of the extra degrees of freedom, the ensemble sampled by such MD methods is not, strictly speaking, the canonical (NVT) ensemble, but rather the NVT $\vec{J}$ ensemble with $\vec{J} = \vec{0}$. This difference may seem unimportant, or even academic, but should be noted when dealing with phase space averages for small molecules. More generally, this topic is relevant in unimolecular reactions or dissociations, where microcanonical or canonical integrals must be evaluated.

In this article, we compare the predictions of molecular dynamics and Monte Carlo methods, for two Hamiltonian systems which model Ar_3 and Ar_3^+, respectively, in both the microcanonical and canonical ensembles. The two molecules illustrate very different kinds of structures, originating from either loosely bound (van der Waals) or strongly bound forces. As such, they can be seen as representative of the various interactions usually found in molecular systems. Our main results are that sampling the configuration space of these small atomic clusters can be very difficult with MD simulations, and

* To whom correspondence should be addressed.

10.1021/jp013691+ CCC: $22.00
Published on Web 03/29/2002

also that angular momentum conservation strongly affects the equilibrium statistical distribution, especially for very asymmetric molecules. To achieve more ergodic MD sampling, we show that a Monte Carlo scheme can be used to generate the suitable initial conditions of the trajectories.

The paper is organized as follows. In the next section, we recall the basic principles of simple MD and MC methods in the microcanonical and canonical ensembles, and we emphasize how to include the conservation of angular momentum in Monte Carlo simulation. In Section III, we study in detail the cases of Ar_3 and Ar_3^+ modeled by a simple classical and a more accurate quantum potential energy function, respectively. The effect of angular momentum conservation on two observables, the kinetic temperature and the instantaneous Lyapunov exponent of Ar_3, is studied in a wide energy range. We also compare the various sampling schemes on a more physical observable for Ar_3^+, namely, the absorption spectrum, and we calculate the average kinetic energy released during unimolecular dissociation of an argon atom from Ar_4 and Ar_4^+, respectively. Finally, we give concluding remarks in Section IV.

II. Sampling Techniques

A. Molecular Dynamics. In the microcanonical ensemble sampling, the usual Newtonian equations of motion have been solved using a fifth-order Adams−Moulton numerical integrator. The initial conditions were taken at the lowest energy configuration with a choice of random initial velocities which satisfy the three mechanical conditions: (a) total energy is E, (b) total linear momentum $\vec{P}$ is zero, and (c) total angular momentum $\vec{J}$ is zero. Step c requires one to invert the inertia matrix, which is only possible for a nonlinear molecule. In the case of Ar_3^+, we slightly shifted one atom off the axis with a small amplitude, therefore not affecting the total energy significantly.

Sampling the configuration space at constant temperature was achieved by molecular dynamics using Nosé−Hoover chains.[2] The equations of motion are now[8]

$$\begin{aligned}
\dot{q}_i &= \frac{p_i}{m_i} \\
\dot{p}_i &= -\frac{\partial V}{\partial q_i} - p_i \upsilon_{\eta_1} \\
\dot{\eta}_i &= \upsilon_{\eta_i} \\
\dot{\upsilon}_{\eta_i} &= \left[\sum_{i=1}^{3N} \frac{p_i^2}{m_i} - (3N-6)k_B T\right] - \upsilon_{\eta_1}\upsilon_{\eta_2} \\
\dot{\upsilon}_{\eta_1} &= [Q_{j-1}\upsilon_{\eta_j-1}^2 - k_B T] - \upsilon_{\eta_j}\upsilon_{\eta_j+1} \qquad 1 < \boldsymbol{j} < \boldsymbol{M} \\
\dot{\upsilon}_{\eta_M} &= Q_{M-1}\upsilon_{\eta_{M-1}}^2 - k_B T
\end{aligned} \tag{1}$$

where $\{q_i\}$, $\{p_i\}$ are the respective coordinates and momenta of the N atoms, and $\{\eta_i\}$ and $\{\upsilon_{\eta_i}\}$ are the respective coordinates and velocities of the M thermostats of the chain. Following Martyna, Klein, and Tuckerman,[8] the thermostat masses were chosen to be $Q_1 = (3N-6)k_BT/\omega^2$ and $Q_j = k_BT/\omega^2$ for $j > 1$, ω being a typical frequency of the system found after diagonalizing the mass-weighted Hessian matrix at the lowest-energy structure. The initial conditions were chosen simply at this geometry without any nonzero velocity except for the thermostat variables. Simple symmetry arguments[9] show that an initial angular momentum set to zero in the simulations is conserved by the above equations of motion. This was previously noticed by Weerasinghe and Amar in a study of cluster evaporation[10] but does not hold for nonzero $\vec{J}$. As a consequence, only the $3N-6$ internal vibrational degrees of freedom are thermalized in the Nosé−Hoover chains method, out of $3N$. This explains the $3N-6$ factor in the rhs of eq 1.

As will be seen in the next section, this conservation can lead to some deviations with respect to the actual canonical ensemble sampling. Nosé−Hoover chains are one straightforward extension of the original extended-ensemble formalism introduced by Nosé and Hoover.[11] As shown by Martyna, Klein, and Tuckerman,[8] more than one thermostat are required for simple oscillators to behave in an ergodic way. A possible alternative consists of using quartic feedback forces for the thermostat variables, as recently suggested by Hoover and coworkers.[12]

B. Monte Carlo. The Metropolis scheme was used for single-temperature (or energy) simulations. The sampling of the statistical distribution $\rho(\Gamma)$ of phase space points Γ is conventionally done by alternating random moves from Γ_{old} to Γ_{new} and by accepting these moves with probability $\mathrm{acc}(\Gamma_{old} \rightarrow \Gamma_{new}) = \min[1, \rho(\Gamma_{new})/\rho(\Gamma_{old})]$. For an atomic system, the statistical distribution ρ can be factorized into configuration- and momenta-dependent parts. In the canonical ensemble, ρ is simply proportional to the Boltzmann factor $\rho_{NVT}(\mathbf{R}) = e^{-\beta V(\mathbf{R})}$, $V(\mathbf{R})$ being the potential energy at configuration $\mathbf{R}$ and $\beta = 1/k_BT$ the inverse temperature. In the microcanonical ensemble and up to a normalization constant, ρ is given by[13]

$$\rho_{NVE}(\mathbf{R}) = [E - V(\mathbf{R})]^{(3N/2-4)}\Theta[E - V(\mathbf{R})] \tag{2}$$

where Θ stands for the step function $\theta(x) = 0$ if $x < 0$, $\theta(x) = 1$ otherwise. Sampling the microcanonical ensemble using Monte Carlo techniques was previously proposed in a rigorous fashion by Schranz, Nordholm, and Nyman[14] following the pioneering work of Severin and co-workers,[15] even though these authors were not specifically interested in the ergodicity matters. Simulations were also performed starting with the lowest-energy configuration and doing individual moves with a step size adjusted to yield between 40% and 60% accepted MC moves.

It is possible to include conservation of angular momentum in the expressions of the equilibrium densities ρ_{NVT} and ρ_{NVE}. One finds[4,5,16]

$$\begin{aligned}
\rho_{NVT}(\mathbf{R}, \vec{J} = \vec{0}) &\propto \frac{\rho_{NVT}(\mathbf{R})}{\sqrt{\det \mathbf{I}(\mathbf{R})}} \\
\rho_{NVE}(\mathbf{R}, \vec{J} = \vec{0}) &\propto \frac{\rho_{NVE}(\mathbf{R})}{\sqrt{\det \mathbf{I}(\mathbf{R})}}
\end{aligned} \tag{3}$$

$\mathbf{I}(\mathbf{R})$ being the inertia tensor of configuration $\mathbf{R}$. The two above equations are only valid for nonlinear molecules. In the systems keeping a linear shape, $\sqrt{\det \mathbf{I}}$ should be replaced by $\mathbf{I}(\mathbf{R})$, and the number of independent degrees of freedom should also drop by one. For a larger, nonlinear molecule, the extra geometrical factor $1/\sqrt{\det \mathbf{I}}$ exhibits small variations in the range of available configuration space. However, not including it can cause some quantitative[6,17] or even qualitative[5] disagreement with molecular dynamics data.

III. Test Cases: Ar_3 and Ar_3^+

For the two systems studied, $N = 3$ atoms and all simulations consisted of 10^3 different initial conditions and 10^4 time steps (MD) or Monte Carlo cycles. The first 10% of the collected data were rejected for equilibration, and only one MC step every

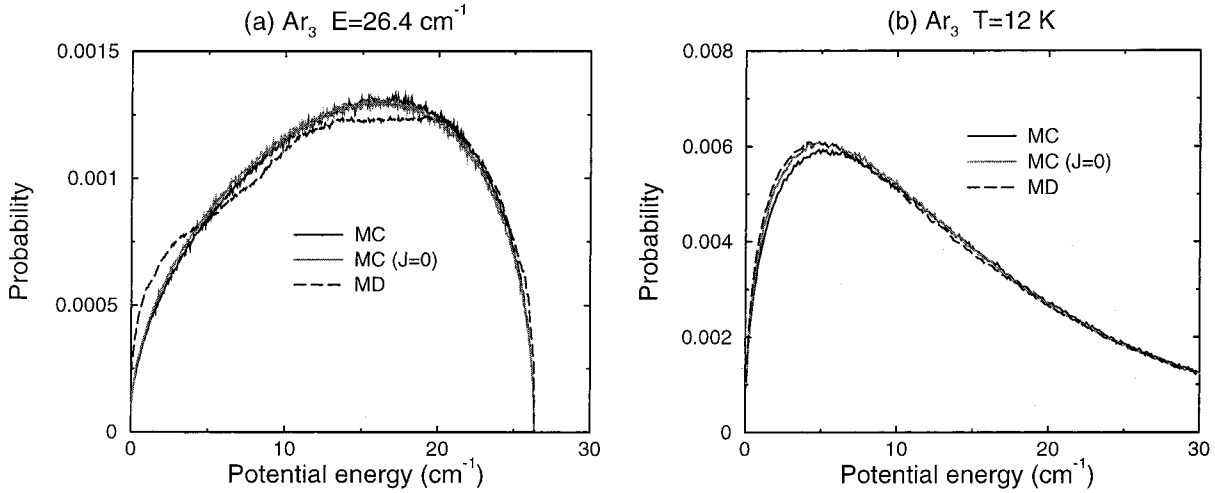

Figure 1. Potential energy distribution of Ar_3 from Monte Carlo simulations with ($J = 0$) and without conservation of angular momentum and also from molecular dynamics simulations. (a) Microcanonical ensemble at total energy $E = 26.4$ cm^{-1}; (b) canonical ensemble at temperature $T = 12$ K.

N steps was included in the Monte Carlo sample to avoid excessive correlations.

A. Ar_3. The simple Lennard-Jones (LJ) potential was employed to model the interaction within neutral Ar_3. We did not need more accurate descriptions for the present statistical purposes. With the usual parameters (for argon) $\epsilon = 172.4$ cm^{-1}, $\sigma = 3.405$ Å, the only equilibrium geometry is an equilateral triangle with length σ and energy -3ϵ. The harmonic zero-point energy, calculated from the three vibrational frequencies at this minimum, is ZPE $= 26.4$ cm^{-1} above this minimum. At constant temperature, the molecular dynamics simulations used a time step of $\delta t = 1$ fs. At constant total energy, we were able to get a good conservation of the mechanical quantities using a larger time step, $\delta t = 10$ fs.

We have plotted in Figure 1a the probability distribution of potential energy found in microcanonical simulations with (MC and MD) and without (MC) angular momentum conservation, at total energy corresponding to the zero-point energy. While the two Monte Carlo distributions can hardly be distinguished, the molecular dynamics results show a somewhat irregular pattern, especially at low and intermediate energies. Repeating the computations with different sets of initial conditions produced the same MC curves, but still a badly converged MD distribution, especially in the case of fewer but longer simulations. This poor convergence of molecular dynamics is the signature of regular orbits and only moderate chaos and will be explored further below.

At the total energy of 26.4 cm^{-1} the kinetic temperature was estimated to be around 12 K, the value which was chosen for the canonical simulations. The results of MC and MD have been represented in Figure 1b, again with and without angular momentum conservation. Only one thermostat variable was used in the Nosé−Hoover chain, but we now find a much better agreement between MC and MD data, although some small disagreement can still be seen between the two MC distributions. Therefore, the constant temperature MD simulation seems to be ergodic thanks to the extra degree of freedom. We checked the stability of the present MD results by performing simulations with a larger number of thermostat variables.

The previous results show that neglecting angular momentum conservation only affects low energy or temperature sampling in small amounts. We have also performed a series of simulations in a wide range of total energies. When the cluster is hot enough, the linear saddle configuration located about 170 cm^{-1} above the minimum can be crossed and spontaneous isomerization between two equivalent triangular shapes (but with different labelings of the atoms) can occur. Isomerization in Ar_3 can be seen as the precursor to the so-called "phase changes" seen in larger clusters such as Ar_{13}.[18] To estimate the influence of the extra factor $1/\sqrt{\det \mathbf{I}(\mathbf{R})}$ on the thermodynamic behavior, we have calculated two specific indicators which can be sensitive to changes in geometry, hence in $\mathbf{I}(\mathbf{R})$. The first indicator is simply the kinetic temperature:

$$T_K(E) = \frac{2\langle K\rangle(E)}{(3N-6)k_B} \tag{4}$$

where the average of the kinetic energy $\langle K\rangle$ is a microcanonical one. When isomerization occurs, the cluster spends relatively long times near the saddle configuration, which results in a decrease of the kinetic temperature. The general shape of the cluster is then characterized by very large values of $1/\sqrt{\det \mathbf{I}}$. In Figure 2a, we see that the variations of T_K with respect to energy are significantly changed by whether we consider this weight or not in the Monte Carlo sampling scheme. The deviations become notably large below the onset of isomerization and increase even further at higher energies.

The second observable computed here is a finite-time Lyapunov exponent. Lyapunov characteristic exponents (LCEs) can contain a lot of information related to the topography of the potential energy surface, as they probe the different convexities of this surface near a minimum and near a saddle point. While calculating LCEs is in principle a purely dynamical task, recent analytical theories[19] have been developed for high-dimensional Hamiltonian systems. These theories give estimates of the LCEs as functions of various geometrical parameters such as the Gaussian curvature, its mean, and its variance values. They have been previously used in the context of clusters,[20] but they were much less accurate for small systems. A complementary approach is that of short-time LCEs. In the limit of infinitely short times, Wales and Berry[21] have found an exact, simple expression for the local Lyapunov exponents $\{\lambda_j\}$:

$$\lambda^2_j = \max_{\omega_j^2<0}(-\omega_j^2, 0) \tag{5}$$

In the above expression, the ω_j^2 are the eigenvalues of the mass-weighted Hessian matrix at the current configuration. Only

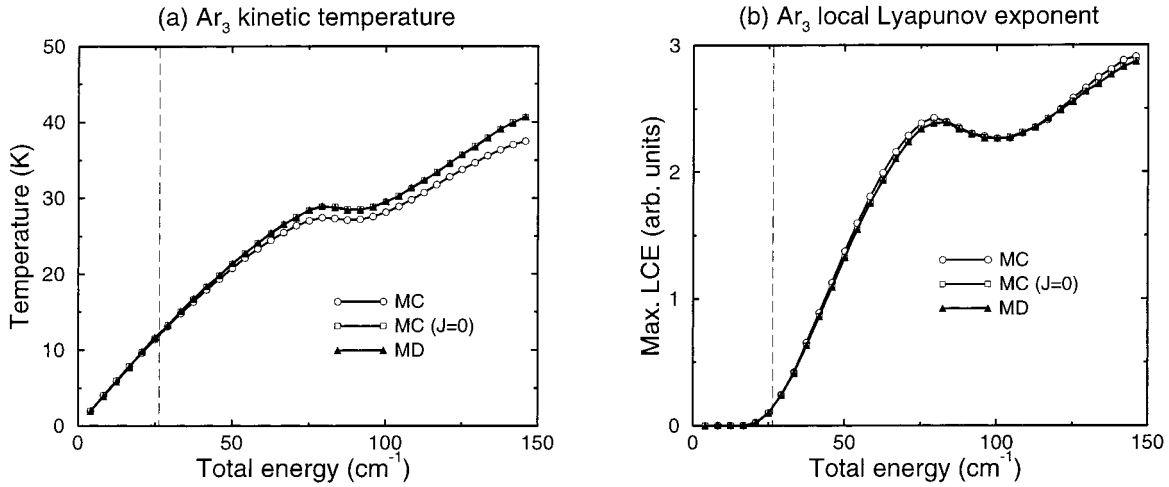

Figure 2. Variations of some statistical observables with total energy in microcanonical simulations of Ar_3, from MC and MD. (a) Kinetic temperature; (b) local largest Lyapunov exponent. The vertical line marks the zero-point energy, 26.4 cm^{-1}.

one specific aspect of Lyapunov instability is accounted for here, namely, the existence of negative curvature of the potential energy surface. Other contributions such as the fluctuations of positive curvature[19] are neglected. However, for small systems eq 5 was seen to yield a reasonable approximation of the large-time, asymptotic Lyapunov exponents by averaging over many instantaneous values.[21,22] Here, we have measured both by the MD and MC methods the largest local Lyapunov exponent Λ in the microcanonical ensemble:

$$\Lambda(E) = \langle \max_j \sqrt{\max_{\omega_j^2<0}(0, -\omega_j^2)} \rangle \qquad (6)$$

The results for Ar_3 are plotted in Figure 2b. The general shape is similar to the "exact" largest Lyapunov exponent calculated by Yurtsever[23] and Calvo[24] and also bears some great resemblance with the Kolmogorov entropy calculated by Hinde, Berry, and Wales.[22] Below some threshold energy, no instability is seen and $\Lambda = 0$. The onset of chaos, when the KAM theorem appears to be no longer valid, is located near 20 cm^{-1} above the minimum energy. Λ then increases and shows a plateau or even a small drop at the isomerization energy, and increases further at higher energy. The drop in Λ has been previously interpreted by Wales and Berry as resulting from the momentary greater harmonicity as the cluster is likely to be located more often (or with a larger probability) near the saddle point.[21] As for the kinetic temperature, we observe some disagreement between the results with and without angular momentum conservation. However, and to our surprise, this disagreement is small compared to the kinetic temperature itself. Thus, even for a system as small as three atoms these results show that molecular dynamics samples the configuration space in an ergodic way at high energy and that the microcanonical ensemble is essentially identical to the molecular dynamics ensemble, once the trajectories have become chaotic enough. At the zero-point energy, the largest Lyapunov exponent is only slightly larger than zero, hence the longer time required for ergodic convergence.

B. Ar_3^+. The charge in Ar_3^+ clusters is delocalized, and a realistic model must include these quantum effects at the atomic level. A relatively simple approach is found in the so-called diatomic-in-molecules (DIM) approximation.[25] We refer the reader to the article[26] for further details on the DIM method. The full description of the parameters used here is given in ref 27. In particular, the interaction between neutral atoms is described by the semiempirical potential of Aziz.[28]

In a previous work on Ar_3^+, Bastida and Gadéa[27] already noticed the presence of periodic orbits and poor ergodicity of this system when modeled with the Foreman potential.[29] However, with the present Aziz potential, a reasonable convergence of the absorption spectra could be obtained from MD simulations at constant total energy. The initial conditions were generated by very slightly distorting the global minimum geometry so that the inertia matrix could be inverted and a set of velocity vectors could yield the total energy required without any global linear momentum or any global angular momentum. The time step used was taken as 1 fs in both the constant energy and constant temperature MD runs.

In contrast with Ar_3, there is an added interest in studying charged systems, as they are much more conveniently produced experimentally. Moreover, the DIM approach allows one to calculate new physical observables of spectroscopic type, which are also more readily accessible in measurements. The potential energy surface of Ar_3^+ is very different from that of Ar_3, and the ground-state geometry of Ar_3^+ is that of a linear molecule, with effective Coulombic charge of $0.5e$ on the center atom and $0.25e$ on each other atom. The atoms are also much more tightly bound to one another in Ar_3^+, the ZPE being about 225 cm^{-1}.

The equilibrium distributions of potential energy in both the microcanonical and canonical ensembles have been plotted in Figures 3a and b. The canonical temperature, $T = 100$ K, is close to the kinetic temperature in microcanonical ensemble runs. Compared to Ar_3, we now observe a much larger disagreement between MD and MC results and between the two MC results with and without angular momentum conservation. First, the microcanonical MD distribution exhibits strong irregularities which again reveal the existence of periodic trajectories. Even by adding one thermostat variable, molecular dynamics remains somewhat nonergodic, since at least two thermostats are needed to get agreement with MC results at constant $\vec{J} = \vec{0}$. Conservation of angular momentum plays here a greater role, simply because the molecule is nearly linear. Therefore $1/\sqrt{\det \mathbf{I}}$ has very large variations, that is, several orders of magnitude.

We have also simulated the absorption spectra of Ar_3^+ using the different samplings above. The absorption spectrum is calculated following semiclassical ideas.[27,30] In a histogram corresponding to energy differences from the ground electronic state to the various excited states, a quantity proportional to

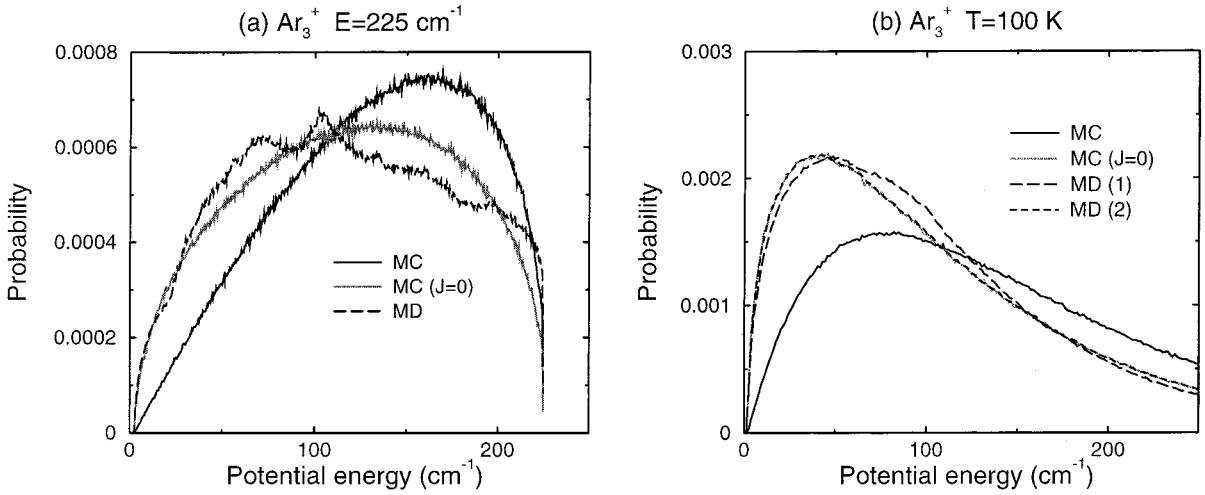

Figure 3. Same as Figure 1 for Ar_3^+. (a) Microcanonical ensemble at total energy $E = 225$ cm^{-1}; (b) canonical ensemble at temperature $T = 100$ K.

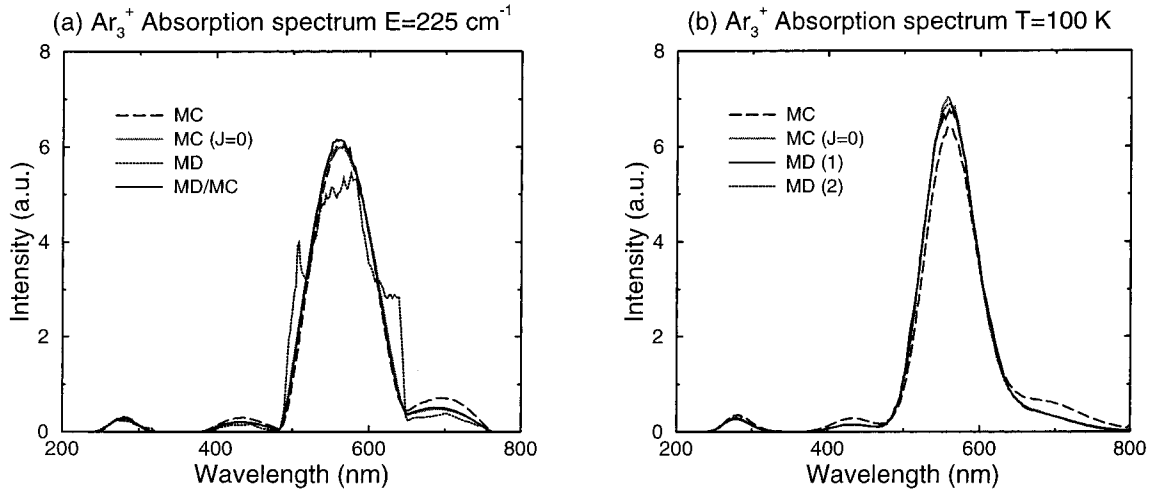

Figure 4. Absorption spectra of Ar_3^+ from MC and MD samplings. (a) Microcanonical ensemble at total energy $E = 225$ cm^{-1}; (b) canonical ensemble at temperature $T = 100$ K.

the absorption efficiency is accumulated using a set of geometries which sample the selected characteristic ensemble. We refer the reader to articles 27, 30, and 31 for further details on this subject.

The different Monte Carlo and molecular dynamics samplings induce some changes in the absorption spectrum, as can be seen in Figure 4. The nonergodic character of microcanonical MD simulation is reflected in these curves, as the four absorption peaks may again show very irregular patterns. The two peaks at 430 and 700 nm are the most sensitive to the sampling of configuration space near the linear geometry, and the intensity gets 20−40% lower if we include conservation of $\vec{J}$.

To reduce the ergodicity problems of MD simulations in the microcanonical ensemble, we have implemented a hybrid MD/MC approach where the initial conditions of MD are taken from a MC run at the same total energy and $\vec{J} = \vec{0}$. The initial velocities are randomly chosen to yield the total energy and linear and angular momenta wanted. The absorption spectrum obtained this way is much closer to the Monte Carlo results, as can be seen in Figure 4a. The regions of phase space visited by the corresponding trajectories are more chaotic than those starting exactly at the equilibrium geometry. To further support these results, we have compared in Figure 5 the distributions of the largest Lyapunov exponent calculated along the 10^3 trajectories. These numbers have been estimated by solving the tangent space equation of motion in the usual way,[32] but not by accumulating the instantaneous exponents as was made above. The two distributions clearly show that the trajectories starting at the equilibrium geometry are much less chaotic than those where the initial conditions are sampled in a ergodic way.

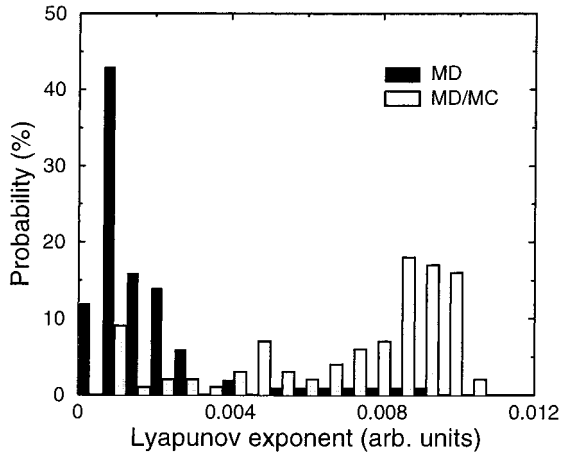

Figure 5. Probability distributions of largest Lyapunov exponent from MD simulations of Ar_3^+ at total energy $E = 225$ cm^{-1}, with initial conditions starting at the global minimum (MD) or taken from set of MC configurations (MD/MC).

The poorly ergodic cases studied here could be quite general. Nonergodic behavior can be quite easily identified. Quasiergodicity, on the other hand, may be much more difficult to detect. Even when convergence seems to have been reached, different pictures could emerge from, for instance, different sets of initial conditions. The absorption spectrum obtained from constant energy MD simulations at 225 cm^{-1} did not converge correctly in the present work, while the alternate choice of initial conditions used by Bastida and Gadéa seems to have worked quite well for the same statistics.[27] Therefore, the usual warning of difficulty in reaching converged observables does not apply systematically. Quasiergodicity, as illustrated here for a small system, could also be the rule rather than the exception for short-time dynamics in larger molecules, often driven by local interactions.

C. Statistics of Unimolecular Dissociation. Phase space integrals are a common ingredient in the calculation of reaction rates or in the distribution of energy released during dissociation. The simple monomer evaporation from Ar_n^{q+} with $q = 0$ or 1 is a barrierless process,

$$Ar_{n+1}^{q+} \rightarrow Ar_n^{q+} + Ar$$

and the product molecule Ar_n^{q+} is the transition state. One can estimate such quantities using various statistical theories (for a review, see ref 33, for instance). The evaluation of absolute evaporation rates is usually difficult because most of the prefactors are unknown a priori. Another physical observable which involves a smaller number of parameters or functions is the average kinetic energy release (KER). Most importantly in the present work, this quantity is closely related with the thermodynamics of the parent cluster.

We have employed three distinct statistical theories to give estimates of the KER at various total energies of the reactant. These theories will not be described in detail, as this is not the purpose of the present article. The Rice−Ramsperger−Kassel (RRK) theory assumes that the dissociating molecule is a ν-dimensional harmonic oscillator and that evaporation corresponds to the breaking of one harmonic bond. In the RRK theory, the average KER $\langle\epsilon\rangle$ (E) at total energy E of the reactant system is given by

$$\langle\epsilon\rangle_{RRK}(E) = \frac{E - E_0}{\nu} \tag{7}$$

In this equation, E_0 is the dissociation energy and $\nu = 3n - 3$. Phase space theory (PST), in the sense of Chesnavich and Bowers,[34] includes the restriction in the phase space integrals because of the rotation of the product. Parneix, Amar, and Bréchignac[35] have shown that a good approximation to the rotational density of states (DOS) $\Gamma(\epsilon, \vec{J} = \vec{0})$ is given by the kinetic energy ϵ of the fragment, up to a multiplicative constant.[36] This leads to the expression for the average KER:[35,36]

$$\langle\epsilon\rangle_{PST}(E) = \frac{\int_0^{E-E_0} \epsilon^2 \Omega_n(E - E_0 - \epsilon)\mathrm{d}\epsilon}{\int_0^{E-E_0} \epsilon \Omega_n(E - E_0 - \epsilon)\mathrm{d}\epsilon} \tag{8}$$

where $\Omega_n(E)$ is the vibrational DOS of the (nonrotating) product molecule. The function Ω_n can be calculated from simulations of the product molecule, either in the microcanonical or canonical ensembles, by the multi-histogram method.[5] This method requires one to perform several simulations at various total energies or temperatures and to build Ω_n from the overlapping potential energy distributions. The calculation of $\langle\epsilon\rangle_{PST}$ thus offers a direct way to compare the microcanonical and molecular dynamics ensemble samplings.

Alternatively, a simple analytical expression for $\langle\epsilon\rangle$ is found by simplifying the above densities of states in the PST equation by their harmonic approximation. This is the basis of the Engelking and Weisskopf models:[37]

$$\langle\epsilon\rangle_{Engelking}(E) = 2\frac{E - E_0}{\nu - 1} \tag{9}$$

The Engelking prediction can be used to quantify the extent of harmonicity in the product molecule by comparing its value to the PST estimate. As seen in previous works,[10,35,38] calculating the average KER can reveal the existence of phase changes, provided that a proper estimation of the vibrational DOS is made first.

For each system investigated previously, we have performed a series of 30 MC simulations at constant energies, up to 150 cm^{-1} for Ar_3 and 800 cm^{-1} for Ar_3^+, and we have calculated the vibrational DOS. Then, the average kinetic energy release in the reactions $Ar_4^{q+} \rightarrow Ar_3^{q+} + Ar$, $q = 0$ or 1, has been estimated using the RRK, PST, and Engelking statistical rate theories. The results are represented in Figure 6 for the two molecules. Phase space theory is known to be fairly accurate with respect to the statistics gathered from actual molecular dynamics simulation of the evaporation process, as shown by Weerasinghe and Amar in argon clusters[10] or more recently by Calvo in C_{60} clusters.[38] As was also seen in these works, the RRK value strongly underestimates both the PST and Engelking predictions.

The average kinetic energy release in the dissociation of Ar_4 follows the same qualitative behavior as the kinetic temperature of Ar_3, with a small backbending at the isomerization threshold near 90 cm^{-1}. The effect of including the conservation of angular momentum in the phase space sampling has the same magnitude as in Figure 2 and gets notable as the cluster starts to isomerize. The deviation from the harmonic line of the Engelking value becomes apparent near 30 cm^{-1}, which is consistent with the rise in the Lyapunov exponent of Figure 2b.

The average kinetic energy released in the dissociation of Ar_4^+ into $Ar_3^+ + Ar$ is much larger, which simply reflects the stronger bonding of this molecule. The difference between the two sampling schemes shows again that conservation of angular momentum has the effect of increasing harmonicity. However, the reasons for this increase are different for the two molecules. Angular momentum conservation favors the linear configuration of Ar_3^{q+}, which is a saddle point for Ar_3, but the equilibrium structure of Ar_3^+. In the former case, harmonicity increases as the system gets close to the saddle point, as previously shown by Wales and Berry.[21] On the contrary, distortions from the linear geometry are disfavored at low energies in Ar_3^+, and harmonicity is further reinforced. As can be seen in Figure 6b, even at 800 cm^{-1}, Ar_3^+ behaves in a quite harmonic way. This is in agreement with the observed regular trajectories in molecular dynamics simulations and the difficulty to achieve ergodicity in this system.

IV. Discussion and Conclusion

From a conceptual point of view, isolated finite atomic or molecular systems are conveniently studied at constant total energy rather than at constant temperature. Because the molecular dynamics approach closely mimics the actual physical behavior, it may be thought to be more accurate in providing a

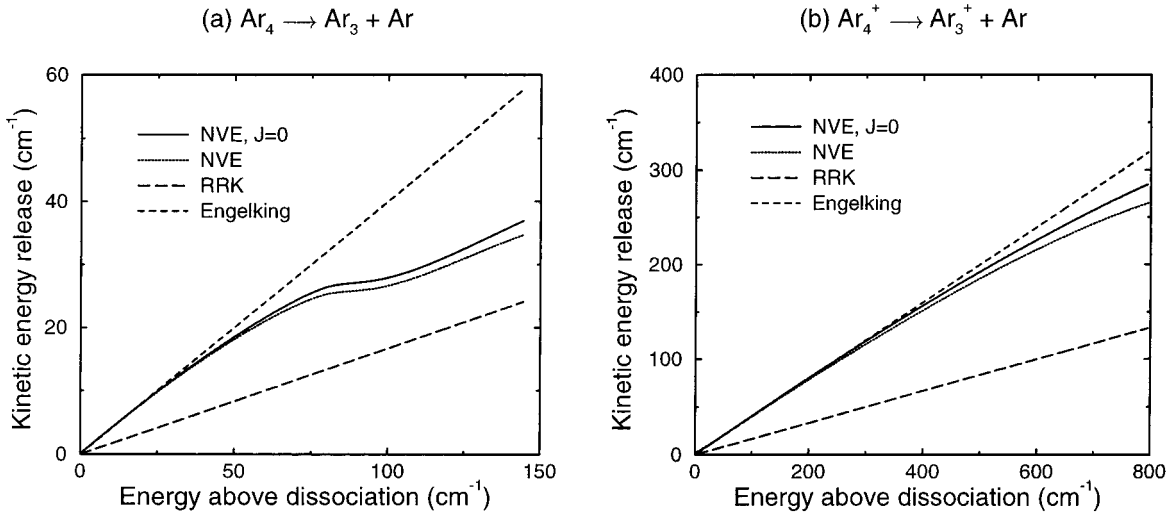

Figure 6. Average kinetic energy release during monomer evaporation in the reactions (a) $Ar_4^+ \rightarrow Ar_3^+ + Ar$; (b) $Ar_4 \rightarrow Ar_3 + Ar$. For each panel, the two straight lines are the predictions of the RRK and Engelking theories, respectively. The two other curves are the result of phase space theory using the vibrational densities of states from Monte Carlo microcanonical sampling in the NVE and NVE $\vec{J} = \vec{0}$ ensembles.

representative set of configurations than nondeterministic, stochastic methods. However, the typical time required for convergence can be approximated as the Lyapunov time $\tau = 1/\Lambda$. Therefore at low energies, τ may rise to very large values or even to infinity in the KAM regime. This can cause some major limitations for MD simulations to reach convergence, as was seen in the present work. Our two examples, Ar_3 and Ar_3^+, have only a modest number of degrees of freedom, but they both show such nonergodic properties at low (but physically sound) energies. In our examples, the statistical data was gathered over 10^3 independent initial conditions and accumulated over 10^4 steps each. If only one initial condition had been chosen, the disagreement between MC and MD data would have been worse. In fact, a 10^7-time steps long MC simulation converges exactly the same way, but the unique MD trajectory can remain close to a periodic orbit, therefore preventing ergodic convergence. Moreover, such long trajectories can raise problems for the accurate conservation of mechanical quantities.

In the two cases presently investigated, only one basin of the potential energy surface is accessible, and standard Monte Carlo simulation can easily produce ergodic sampling. Nevertheless, MC and MD predictions could be brought to agreement only if we included conservation of angular momentum in the Monte Carlo scheme. This can be achieved by adding a geometrical factor $1/\sqrt{\det \mathbf{I}}$ to the equilibrium phase space density. In Ar_3^+, this weight $1/\sqrt{\det \mathbf{I}}$ can be especially large near the linear geometry. For Ar_3, some differences in several observables occur when the linear configurations become available.

Strictly speaking, deterministic molecular dynamics at constant energy does conserve all mechanical quantities including angular momentum $\vec{J}$, so do Nosé−Hoover type methods at constant temperature, provided that $\vec{J} = \vec{0}$. The corresponding "NVT $\vec{J} = \vec{0}$" statistical ensemble is somewhat unphysical, as there is no reason the system should keep its angular momentum constant while being thermostated. It appears as a natural restriction because of the use of deterministic MD methods, which will affect the outcome of simulation results for any finite system.

Thus, we expect that sampling the configuration space of linear systems must be done carefully depending on the physical or chemical situation, which may or may not require to keep $\vec{J}$ constant. Obviously, the disagreement between the sampling obtained from MD and the ones from standard MC (i.e., without constant $\vec{J}$) simulations should be less important for larger systems, as linear configurations are less frequent. However, the increasing complexity of the potential energy landscape should also be seen in the much larger number of isomers or stable configurations. The competition between available isomers may yield new nonergodicity or quasiergodicity problems because of the long relaxation time required to cross the barriers separating these isomers. Even stochastic methods, in their basic form, can be very slow in reaching convergence.[39,40] They must be improved using specific techniques such as jump-walking[41] or parallel tempering,[42] which have been shown to be efficient in both the microcanonical and canonical ensembles.[6,43]

Finally, by seeding the molecular dynamics runs with configurations taken from a properly made Monte Carlo simulation within the same statistical ensemble, we have significantly improved the ergodic properties of MD simulations. Of course, this hybrid MD/MC approach is rigorously equivalent to a pure Monte Carlo method in the limit of many infinitely short MD trajectories. In practice, the length of the MD trajectories and the time spent doing MD simulation relative to the time spent doing MC simulation should be adapted to the system under study. When the forces are computationally expensive, Monte Carlo could be a better choice. On the other hand, the dynamics may be faster than MC in some cases. For instance, Car−Parrinello dynamics offers a convenient way to accelerate the computation of the potential energy in the ground electronic state. This method is nevertheless also sensitive to nonergodic troubles.

In the present work, we have focused on nonrotating systems. By emphasizing the possibly important role of angular momentum conservation at $\vec{J} = \vec{0}$, we have studied physical observables that can be amenable to experimental comparison, such as the photoabsorption spectrum or the average kinetic energy released in unimolecular dissociation. This situation is relevant to any molecular system whose vibrational energy is much larger than its rotational energy, as in the experimentally studied Ar_3^+. Rotating systems with constant but nonzero $\vec{J}$ can also be investigated with means of Monte Carlo methods, as first shown by Nyman and co-workers.[4] Constant energy or constant temperature simulations with finite $\vec{J}$ involve the effective rovibrational potential energy surface $V_{\vec{J}}(\mathbf{R}) = V(\mathbf{R}) + \vec{J}^t \mathrm{I}^{-1}(\mathbf{R})\vec{J}/2$ but also the geometrical weight $1/\sqrt{\det \mathbf{I}}$ in

the phase space integrals. A comparison with molecular dynamics data has shown previously that this weight should not be neglected even for quite large systems such as Ar_{13} in the vicinity of the solidlike−liquidlike phase change.[5]

However, and whatever the angular momentum, constant energy molecular dynamics has inherent limitations when several basins of the energy landscape are available but not connected. In this case, the energy barriers higher than the total energy prevent isomerization and hinder ergodicity, which can only be restored by exchange techniques and the use of simultaneous trajectories as in parallel-tempering Monte Carlo.[6]

In conclusion, stochastic simulation methods have several advantages over deterministic molecular dynamics in terms of exploring the configuration space ergodically. These advantages must be balanced with the need for time-dependent observables. At constant temperature, Langevin dynamics offers an interesting alternative to extended ensemble molecular dynamics, even though it is known to be inaccurate at short times. An isolated system, that is, with constant energy but also with linear and angular momentum, still requires standard MD simulations to get explicit dynamical information. A proper use of Monte Carlo methods appears then as the natural choice for selecting the initial conditions.

References and Notes

(1) Allen, M. P.; Tildesley, D. J. *Computer Simulation of Liquids*; Oxford: New York, 1987.

(2) Frenkel, D.; Smit, B. *Understanding Molecular Simulation*; Academic Press: New York, 1996.

(3) Çagin, T.; Ray, J. R. *Phys. Rev. A* **1988**, *37*, 247.

(4) Nyman, G.; Nordholm, S.; Schranz, H. W. *J. Chem. Phys.* **1990**, *93*, 6767.

(5) Calvo, F.; Labastie, P. *Eur. Phys. J. D* **1998**, *3*, 229.

(6) Calvo, F.; Neirotti, J. P.; Freeman, D. L.; Doll, J. D. *J. Chem. Phys.* **2000**, *112*, 10350.

(7) Jellinek, J.; Goldberg, A. *J. Chem. Phys.* **2000**, *113*, 2570.

(8) Martyna, G. J.; Klein, M. L.; Tuckerman, M. *J. Chem. Phys.* **1992**, *97*, 2635.

(9) The angular momentum vector $\vec{J}$ fulfills the equation $d\vec{J}/dt = \vec{M} - \upsilon_{\eta 1}\vec{J}$, where $\vec{M} = -\sum_i \mathbf{r}_i \times (\partial V/\partial \mathbf{r}_i)$ is the total torque of the forces. By rotational invariance, $\vec{M} = 0$, hence $\vec{J}$ remains equal to zero if its initial value and derivative are both set to zero.

(10) Weerasinghe, S.; Amar, F. G. *J. Chem. Phys.* **1993**, *98*, 4967.

(11) Nosé, S. *Mol. Phys.* **1984**, *52*, 255. Hoover, W. G. *Phys. Rev. A* **1985**, *31*, 1695.

(12) Posch, H. A.; Hoover, W. G. *Phys. Rev. E* **1997**, *55*, 6803. Hoover, W. G.; Hoover, C. G.; Isbister, D. J. *Phys. Rev. E* **2001**, *63*, 026209. Hoover, W. G.; Posch, H. A.; Hoover, C. G. *J. Chem. Phys.* **2001**, *115*, 5744.

(13) Pearson, E. M.; Halicioglu, T.; Tiller, W. A. *Phys. Rev. A* **1985**, *32*, 3030.

(14) Schranz, H. W.; Nordholm, S.; Nyman, G. *J. Chem. Phys.* **1991**, *94*, 1487.

(15) Severin, E. S.; Freasier, B. C.; Hamer, N. D.; Jolly, D. L.; Nordholm, S. *Chem. Phys. Lett.* **1978**, *57*, 117.

(16) Dumont, R. S. *J. Chem. Phys.* **1991**, *95*, 9172.

(17) Miller, M. A. Ph.D. Thesis, Cambridge University, 1999.

(18) Jellinek, J.; Beck, T. L.; Berry, R. S. *J. Chem. Phys.* **1986**, *84*, 2783.

(19) Casetti, L.; Livi, R.; Pettini, M. *Phys. Rev. Lett.* **1995**, *74*, 375. Casetti, L.; Clementi, C.; Pettini, M. *Phys. Rev. E* **1996**, *54*, 5969.

(20) Mehra, V.; Ramaswamy, R. *Phys. Rev. E* **1997**, *56*, 2508.

(21) Wales, D. J.; Berry, R. S. *J. Phys. B* **1991**, *24*, L351.

(22) Hinde, R. J.; Wales, D. J.; Berry, R. S. *J. Chem. Phys.* **1992**, *96*, 1376. Hinde, R. J.; Berry, R. S. *J. Chem. Phys.* **1993**, *99*, 2942.

(23) Yurtsever, E. *Europhys. Lett.* **1997**, *37*, 91.

(24) Calvo, F. *J. Chem. Phys.* **1998**, *108*, 6861.

(25) Ellison, F. O. *J. Am. Chem. Soc.* **1963**, *85*, 3540. Tully, J. C. *J. Chem. Phys.* **1976**, *64*, 3182.

(26) Kuntz, P. J.; Valdorf, J. *Z. Phys. D* **1988**, *8*, 195.

(27) Bastida, A.; Gadéa, F. X. *Chem. Phys.* **1996**, *209*, 291.

(28) Aziz, R. A. *J. Chem. Phys.* **1993**, *99*, 4518.

(29) Foreman, P. B.; Lees, A. B.; Rob, P. K. Unpublished results.

(30) Bastida, A.; Gadéa, F. X. *Z. Phys. D* **1997**, *39*, 325.

(31) Galindez, J.; Calvo, F.; Paska, P.; Hrivnak, D.; Kalus, R.; Gadéa, F. X. *Comput. Phys. Comm.* **2002**, in press.

(32) Benettin, G.; Galgani, L.; Strelcyn, J.-M. *Phys. Rev. A* **1976**, *14*, 2338.

(33) Gilbert, R. G.; Smith, S. C. *Theory of Unimolecular and Recombination Reactions*; Blackwell Scientific: Oxford, 1990.

(34) Chesnavich, W. J.; Bowers, M. T. *J. Chem. Phys.* **1977**, *66*, 2306.

(35) Parneix, P.; Amar, F. G.; Bréchignac, P. *Chem. Phys.* **1998**, *239*, 121.

(36) Actually, this result was obtained for the case of a system atom + spherical top, from the relation $\Gamma(\epsilon, \vec{J} = \vec{0}) = J_{max}^2$ between the rotational density of state and the maximum value of the angular momentum of the product molecule. The same relation can be found in a system atom + linear molecule. Thus, the analysis of Parneix and co-workers (ref 35) showing that $\Gamma(\epsilon, \vec{0}) \approx \epsilon$ holds for the linear Ar_4^+.

(37) Engelking, P. C. *J. Chem. Phys.* **1986**, *85*, 3103.

(38) Calvo, F. *J. Phys. Chem. B* **2001**, *105*, 2183.

(39) Thirumalai, D.; Mountain, R. D. *Phys. Rev. A* **1990**, *42*, 4574.

(40) Neirotti, J. P.; Freeman, D. L.; Doll, J. D. *Phys. Rev. E* **2000**, *62*, 7445.

(41) Frantz, D. D.; Freeman, D. L.; Doll, J. D.; *J. Chem. Phys.* **1990**, *93*, 2769.

(42) Swendsen, R. H.; Wang, J.-S. *Phys. Rev. Lett.* **1986**, *57*, 2607.

(43) Neirotti, J. P.; Calvo, F.; Freeman, D. L.; Doll, J. D. *J. Chem. Phys.* **2000**, *112*, 10340.